Ship Motion Prediction in Regular Head Waves

Md. Al Amin Miazee [1*], N.M.G. Zakaria [2]
[1] Dept. of Naval Architecture and Marine Engineering, Sonargaon University (SU)
[2] Dept. of Naval Architecture and Marine Engineering, Bangladesh University of Engineering and Technology (BUET)
*Corresponding Author: Lecturer; Sonargaon University (SU), Dhaka, Bangladesh
Email: alamin.name@su.edu.bd

Abstract

Ship motions are defined by the six degrees of freedom that a ship, boat or any other craft can experience. Heave and pitch are linear and rotational ship motions which are very important in case of regular head waves. This paper presents the prediction of heave and pitch motion of ship in regular head waves. The heaving and pitching motions of a typical ship model are predicted theoretically. Comparison is made between theoretical prediction and experimental results for each vessel. For the validation of the result, a model of series 60 ship has been taken. Heave and pitch motion results have been compared with experimental and other numerical results. A reasonable prediction has been found for this model. A fine destroyer and fuller bulk carrier have been taken also to check their motion results at various Froude numbers. It has been found that the predicted result computed by the present program gives very close to experimental results for the ship with wide range of block coefficient from 0.5 to 0.8.

Keywords: Ship Motion, Regular Waves, Linear Strip Theory, Destroyer.

Nomenclature

a-e, A-E, g, G	Coefficient of equation of motion	ωe	Frequency of encounter
Fr	Froude Number	τ	Phase angle of pitching moment
F0	Amplitude of time-varying heaving force	$\ddot{z}$	Heaving acceleration of center of gravity of ship or model
$\overline{F}$	Complex vertical (heaving) force	z0	Amplitude of heaving motion.
Gw	Gravitational acceleration	$\overline{z}$	Complex heaving motion
CB	Block Coefficient	δ	Theoretically computed heaving phase angle
T	Time	Δ	Displacement of ship or model
P	Density of Water	ε	Theoretically computed pitching phase angle
L	Length of ship or model	θ	Pitching displacement
M	Total pitching moment	$\dot{\theta}$	Pitching velocity

		$\ddot{\theta}$	Pitching accelerations
M0	Amplitude of time-varying pitching moment	θ0	Amplitude of pitching motion
$\overline{M}$	Complex pitching moment	$\overline{\theta}$	Complex pitching motion
N(ζ)	Sectional damping coefficient	λ	Wavelength
Z	Heaving motion of C.G of ship or model	V	Speed of ship or model
$\dot{z}$	Heaving velocity of C.G of ship or model	σ	Phase angle of heaving force

1.0. Introduction

Ship motion prediction is important because it is directly related to the safe and economic operation of the ships. An accurate assessment of ship motions is crucial importance in the process of initial design stage. One important concern is the problem of capsizing in extreme weather conditions. Other concerns include the economic fuel consumption, efficient transfer of pay-loads between marine vehicles, improved performance of tracking devices, improved missile launching capability etc. In the design stage of ships design engineers must consider ship motion. Design engineers can save time and resources by being able to anticipate the ship's performance in early stages.

2-D based theoretical and computational methods of ship motion computations have been under development for over the past 40 years by various researchers such as rational strip theory of Ogilvie et al. (1969) and the new strip theory of Salvesen et al. (1970). One main difference between the different strip theories is the dependence of the coefficients on the forward speed and the treatment of the boundary conditions. In general, all of the strip-theory calculations give satisfactory results for slender-body ships with small amplitude motions, where the nonlinear and three-dimensional effects are insignificant. Many attempts have been made to overcome some of the shortcomings of strip theory. Wang (1976) combined the strip-theory approximation and the dynamic theory to derive the hydrodynamic coefficients of ship motions. The dynamic theory treats the fluid and the body together as one dynamical system. The classical dynamic theory treats the fluid as an unbounded medium, while Wang's formulation takes into account the existence of the free surface. The results of this approach were very similar to those derived by Salvesen et al. (1970). As a matter of fact, the two methods become identical when the interaction between the body and the free surface is neglected. Troesch (1981) used the slender-body theory to derive formulae for the sway, roll, and yaw motion coefficients. Liu et al. (1997) tried to extend the strip theory and apply it to large-amplitude motions. An attempt was done to include some nonlinear effects by taking into account the instantaneous variations of the wetted hull surface during motion and its effects on the ship

hydrodynamic characteristics. The method is a quasi-steady approach, which does not take into account the memory effects. Crossland et al. (1993) conducted a series of experiments to measure the heave and pitch decay-time histories of a model ship. The aim of these experiments was to explain the over prediction of the sectional damping obtained using a strip-theory program. The over prediction of the sectional damping creates poor predictions of free decay motions. This issue has not been resolved completely and it has been concluded that strip theory should be used only in low-amplitude motions when making sea keeping predictions. As mentioned before, many research works are devoted to improving strip-theory predictions, including the applicability to situations where the 3D and nonlinear effects are significant. Earlier prediction methods followed the pioneering works of Korvin-Kroukovsky (1957) and were based on 2D theories. A number of 2D strip-theory based methods of computations were subsequently developed by various researchers.

In this research work 2D linear strip theory by Korvin-Korvosky et al. (1957) has been used to predict hydrodynamic coefficients such as added mass, damping, and exciting force. A computer program has been developed to solve the hydrodynamic coefficients. Then these coefficients were used to solve the motion equations.

2.0. Methodology

2.1. Prediction of Ship Motion Using Linear Strip Theory

Strip theory given by Korvin-Korvosky et al. (1957) has been used for determining the parameters of the ship-motion equations. The predictions are based on 2D evaluations of the ship parameters, whereby the ship is divided into several 2D transverse sections (strips) along the ship's longitudinal axis. These sections are assumed not to interact with each other. The 2D parameters are usually evaluated using potential-flow theories. In strip theory, the 3D-ship-motion coefficients are expressed in terms of integrals of 2D sectional coefficients. These coefficients are then calculated with the assumption that the 2D sections do not interact with each other. To calculate the 2D coefficients Lewis-forms method has been used. In this method, a velocity potential is determined for a cylinder oscillating in an undisturbed free surface in the sway, heave, and roll motions. Bernoulli's equation is then applied to the velocity potential to calculate the pressure distribution on the cylinder. Integration of the pressure yields the added mass and damping forces.

2.2. Analytical details of the Linear Strip theory of ship motions

The coupled set of linear differential equations can be expressed as:

$$a\ddot{z} + b\dot{z} + cz + d\ddot{\theta} + e\dot{\theta} + g\theta = \overline{F} exp(i\omega_e t) \quad (1) \quad A\ddot{\theta} + B\dot{\theta} + C\theta + D\ddot{z} + E\dot{z} + Gz = \overline{M} exp\ (i\omega_e t) \quad (2)$$

Where,

z and θ are the complex heave and pitch vectors,

F and M are wave induced exciting force and moments,

ω_e the frequency of encounter,

a,b,c,d,e,g and A,B,C,D,E,G are the coefficients of the equation of motion.

The above equations result from equilibrium considerations of the hydrodynamic forces and moments called equation of motion, when meeting head or astern regular waves. Following the principles of classical dynamics, these forces and moments are obtained by applying Newton's Second Law of Motion to both translatory and rotational displacements of the body's center of gravity. The wave induced excitation force and moment may be defined as:

$$\overline{F} exp(i\omega_e t) = F_0 exp(-i\sigma)\ exp\ (i\omega_e t) = F_0 exp[i(\omega_e t - \sigma] \qquad (3)$$

$$\overline{M} exp\ (i\omega_e t) = M_0 exp(-i\tau)\ exp\ (i\omega_e t) = M_0 exp[i(\omega_e t - \tau)] \qquad (4)$$

The differential exciting force acting on a control section distant ζ from the origin of the moving coordinate system (ship's C.G.), can be expressed in the simplified form,

$$\frac{dF}{dx} = \frac{dF_1}{dx} cos\ \omega_e t + \frac{dF_2}{dx} sin\ \omega_e t = [\{ \phi_1 sin \frac{2\pi\zeta}{\lambda} + \phi_2 \frac{2\pi h C_W}{\lambda} cos \frac{2\pi\zeta}{\lambda} \} exp (-\frac{2\pi y}{\lambda})] cos\ \omega_e t + [\{\phi_1 cos \frac{2\pi\zeta}{\lambda} + \phi_2 \frac{2\pi h C_W}{\lambda} sin \frac{2\pi\zeta}{\lambda} \} exp (-\frac{2\pi y}{\lambda})] sin\omega_e t \qquad (5)$$

Where,

$$\phi_1 = h\rho g B - \frac{4\pi^2 h C_W}{\lambda^2}(\rho S k_2 k_4) \qquad (6)$$

$$\phi_2 = N(\zeta) - V \frac{d(\rho S k_1 k_2)}{d\zeta} \qquad (7)$$

While the differential exciting moment of this force about the C.G. is given by $\frac{dF}{d\zeta} d\zeta$. Integration of the above two quantities over the ship length results in the values of the total time-varying exciting force and moment, which are considered as the real parts of the Eq. (3) and Eq. (4).

Thus, $F = F_1 cos\ \omega_e t + F_2 sin\ \omega_e t = \sqrt{F_1^{\,2} + F_2^{\,2}} cos\ [\omega_e t - arctan \frac{F_2}{F_1}] = F_0 cos(\omega_e t - \sigma)$ (8)

and, $M = M_1 cos\ \omega_e t + M_2 sin\ \omega_e t = \sqrt{M_1^{\,2} + M_2^{\,2}} cos\ [\omega_e t - arctan \frac{M_2}{M_1}] = M_0 cos(\omega_e t - \tau)$ (9)

The analysis of the forces and moments which correspond to the ship's free oscillations in calm water yields terms which appear on the LHS of the Eq. (1) and Eq. (2). The final expressions

for the coefficients of the equation of motion used in the computations can be found in reference Al Amin et al. (2013).

After algebraic manipulation, the complex heave and pitch amplitude becomes

$$\bar{z} = z_1 - iz_2 = \sqrt{z_1^2 + z_2^2}\exp\left[-i\arctan\frac{z_2}{z_1}\right] \tag{10}$$

$$\bar{\theta} = \theta_1 - i\theta_2 = \sqrt{\theta_1^2 + \theta_2^2}\exp\left[-i\arctan\frac{\theta_2}{\theta_1}\right] \tag{11}$$

Finally $z = R_e\bar{z}\ exp(i\omega_e t) = R_e\sqrt{z_1^2 + z_2^2}exp\ [i(\omega_e t - arctan\frac{z_2}{z_1})] = z_0\cos(\omega_e t - \delta)$ (12)

$$\theta = R_e\bar{\theta}\ exp(i\omega_e t) = R_e\sqrt{\theta_1^2 + \theta_2^2}exp\ [i(\omega_e t - arctan\frac{\theta_2}{\theta_1})] = \theta_0\cos(\omega_e t - \varepsilon) \tag{13}$$

3.0. Validation

For the validation of numerical results given by developed computer program, a Series 60 ship of C_B=0.7 has been taken. The principal particulars of the ship are shown in Table 1. Body plan is shown in Fig.1. Test results have been taken from Gerritsma et al. (1967).

Table 1. Model characterization of series 60 ship.

LWL	2.479m
LBP	2.438m
Beam	0.3481m
Draft	0.139m
LCG	0.0119m (forward of amidships)
C_B	0.70

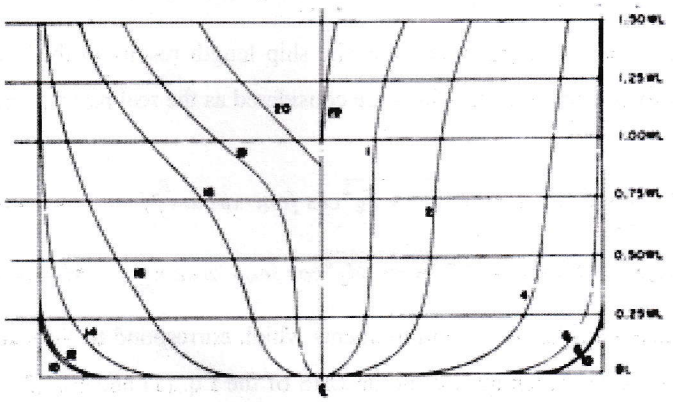

Fig. 1. Body plan of series 60.

Fig. 2, shows the comparison between the calculated results with experimental and other numerical results for heave added mass at Fr = 0.2. From this graph, it is seen that the non-dimensional heave added mass decreases gradually with the increasing value of $\omega_e(L/g)^{1/2}$. The calculated results deviate more at the higher value of $\omega_e(L/g)^{1/2}$ from the experimental results because of increasing wave frequency.

Fig. 3, shows the comparison between the calculated results with experimental and other numerical results for pitch added mass at Fr = 0.2. From this graph, it is seen that the non-dimensional pitch added mass decreases gradually with the increasing value of $\omega_e(L/g)^{1/2}$. But this time the calculated results is too close to the experiment results than the previous one.

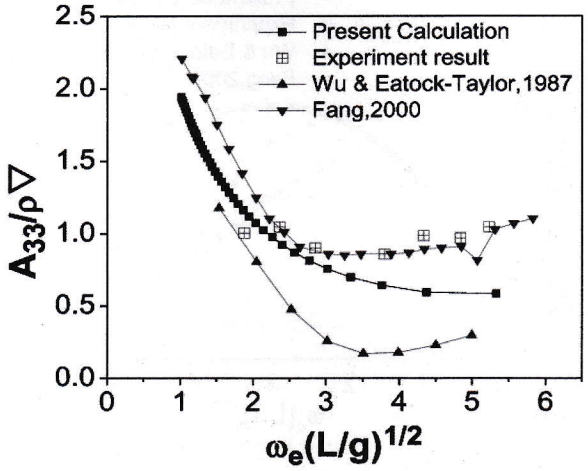

Fig. 2. Heave motion at F_n=0.2 in head sea.

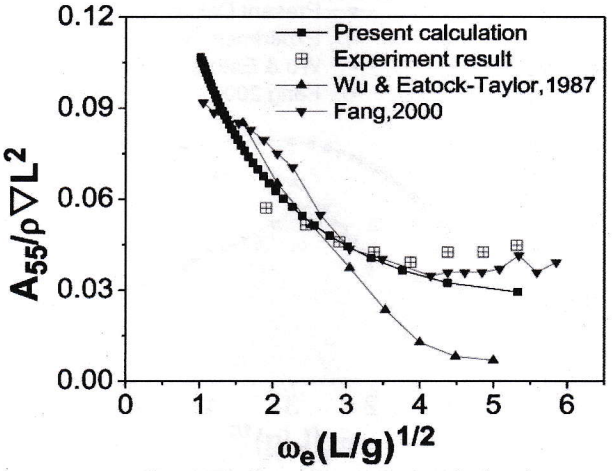

Fig. 3. Pitch motion at F_n=0.2 in head sea.

Fig. 4, shows the comparison between the calculated results with experimental and other numerical results for heave damping at Fr = 0.2. From this graph, it is seen that the non-dimensional heave damping increases gradually with the increase of the value of $\omega_e(L/g)^{1/2}$ and the calculated value deviates more at higher value of $\omega_e(L/g)^{1/2}$ from the experimental value, because of increasing value of wave frequency of encounter.

Fig. 5, shows the comparison between the calculated results with experimental and other numerical results for pitch damping at Fr = 0.2. From this graph, it is seen that the non-dimensional pitch damping increases gradually with the increase of the value of $\omega_e(L/g)^{1/2}$ but the experimental value decreases with increasing wave frequency value.

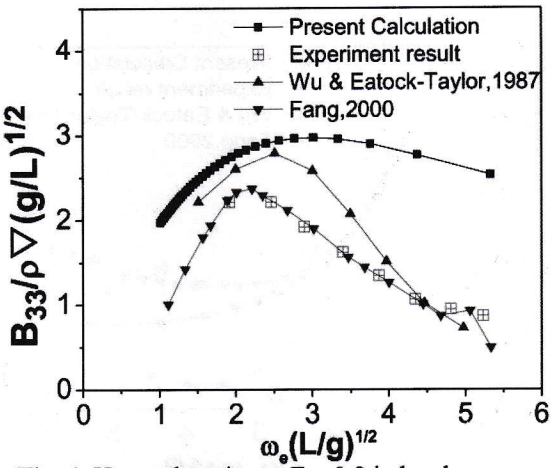

Fig. 4. Heave damping at Fn=0.2 in head sea.

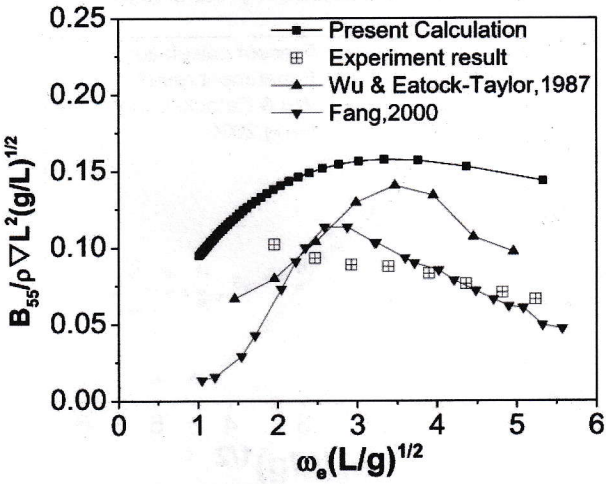

Fig. 5. Pitch damping at F_n=0.2 in head sea.

Fig. 6, shows the comparison between the calculated results with experimental and other numerical results for heave exciting force at Fr = 0.2. From this graph, it is seen that the non-dimensional heave exciting force decreases gradually with the increase of the value of $\omega_e (L/g)^{1/2}$ and the calculated value is very close to the experimental value.

Fig. 7, shows the comparison between the calculated results with experimental and other numerical results for pitch exciting moments at Fr = 0.2. From this graph, it is seen that the non-dimensional pitch exciting moments increases and then decreases gradually with the increase of the value of $\omega_e(L/g)^{1/2}$ and the calculated value is slightly deviates from the experimental value because of resonance.

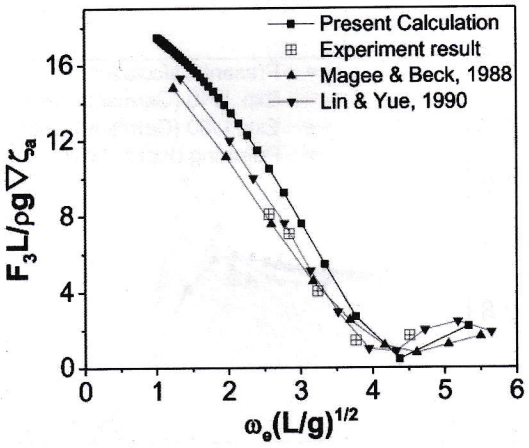

Fig. 6. Heave exciting force at F_n=0.2 in head sea.

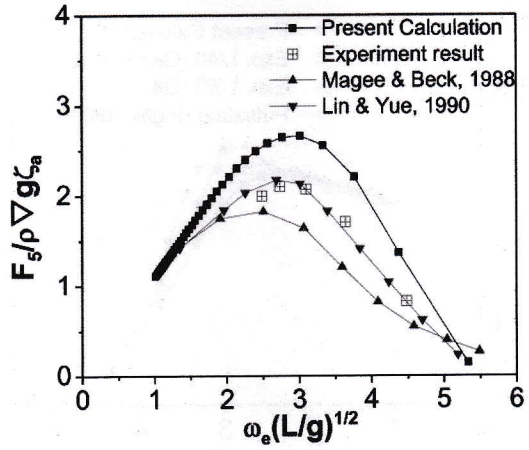

Fig. 7. Pitch exciting force at F_n=0.2 in head sea.

Fig. 8, shows the comparison between the calculated results with experimental and other numerical results for heave motion at Fr = 0.2. From this graph, it is seen that the non-dimensional heave motion increases at a certain limit and then decreases gradually with the increase of the value of $\omega_e(L/g)^{1/2}$ and the calculated value is slightly lower from the pick because of resonance to the experimental value.

Fig. 9, shows the comparison between the calculated results with experimental and other numerical results for pitch motion at Fr = 0.2. From this graph it is seen that the non-dimensional pitch motion increases at a certain limit and then decreases gradually with the increase of the value of $\omega_e(L/g)^{1/2}$ and the calculated value is slightly lower from the pick because of resonance to the experimental value.

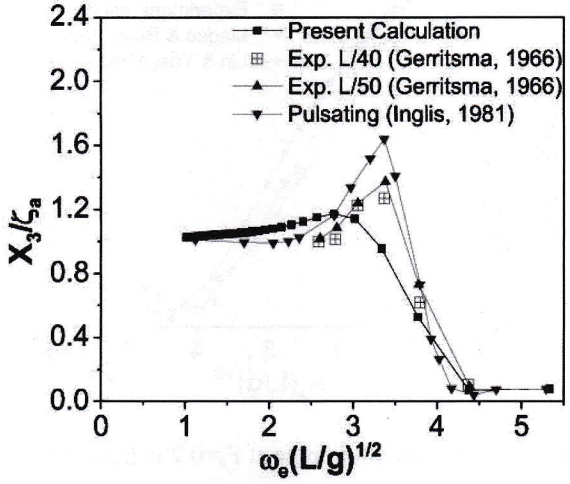

Fig. 8. Heave motion at at F_n=0.2 in head sea.

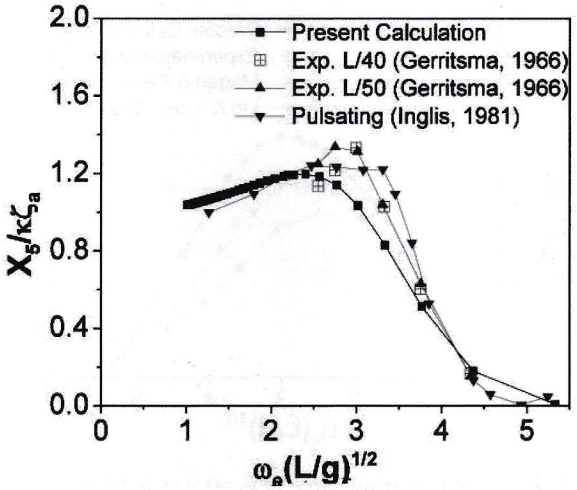

Fig. 9. Pitch motion at at F_n=0.2 in head sea.

4.0. Case Study

For case study two ship of different hull form such as Destroyer and Bulk Carrier have been chosen as follows:

4.1. Case study-1: Destroyer

For the validation of numerical results given by developed computer program, a Destroyer of C_B=0.5374 has been taken. The principal particulars of the ship are shown in Table 2. Body plan is shown in Fig.10. Test results have been taken from Salvesen et al. (1970).

Table 2. Model characteristics of destroyer.

LWL	5.307m
LBP	5.307m
Beam	0.565m
Draft	0.194m
LCG	0.0856m (forward of amidships)
C_B	0.5374

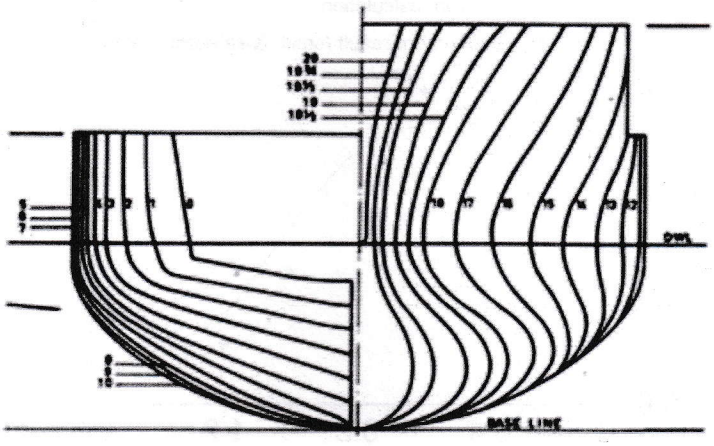

Fig. 10. Body plan of destroyer.

Fig. 11, shows the comparison between the calculated results with experimental results for heave motion at Fr = 0.25. From this graph, it is seen that the non-dimensional heave motion increases at a certain limit and then decreases gradually with the increase of the value of L/λ and the calculated value is slightly lower from the pick because of resonance to the experimental value.

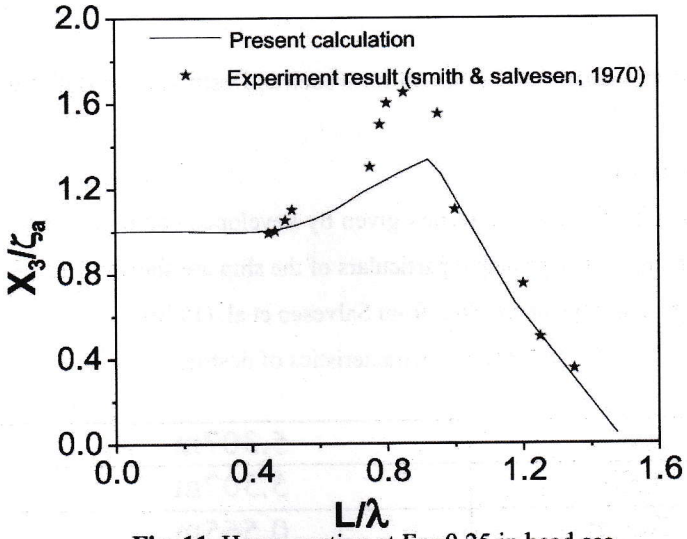

Fig. 11. Heave motion at Fn=0.25 in head sea.

Fig.12, shows the comparison between the calculated results with experimental results for pitch motion at Fr = 0.25. From this graph, it is seen that the non-dimensional pitch motion increases at a certain limit and then decreases gradually with the increase of the value of L/λ and the calculated value is as like as previous.

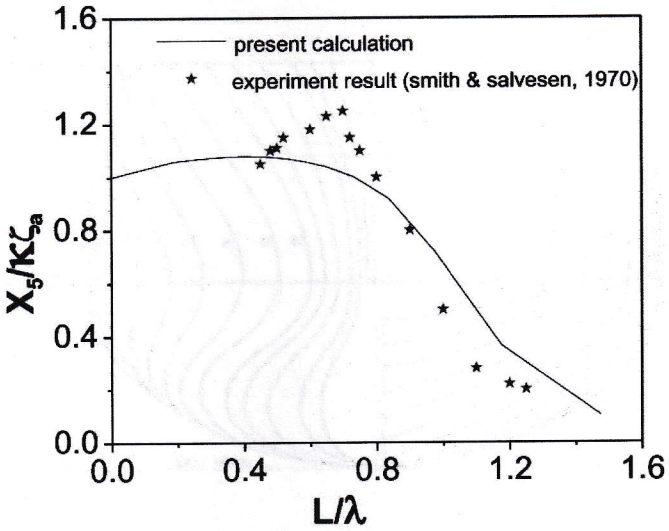

Fig. 12. pitch motion at at Fn=0.25 in head sea.

Fig. 13, shows the comparison between the calculated results with experimental results for heave motion at Fr = 0.35. Fig.14, shows the comparison between the calculated results with experimental results for pitch motion at Fr = 0.35.

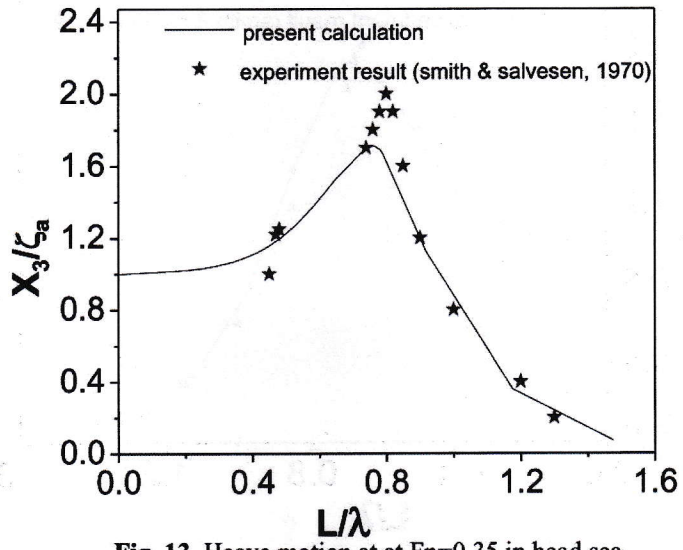

Fig. 13. Heave motion at at Fn=0.35 in head sea.

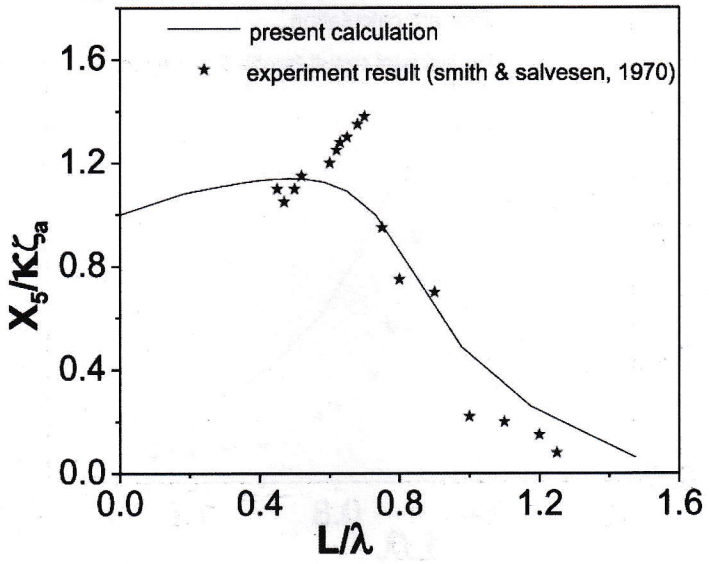

Fig. 14. Pitch motion at at Fn=0.35 in head sea.

Fig. 15, shows the comparison between the calculated results with experimental results for heave motion at Fr = 0.45. From this graph, it is seen that the non-dimensional heave motion increases at a certain limit and then decreases gradually with the increase of the value of L/λ and the calculated value is close to the pick of the experimental value.

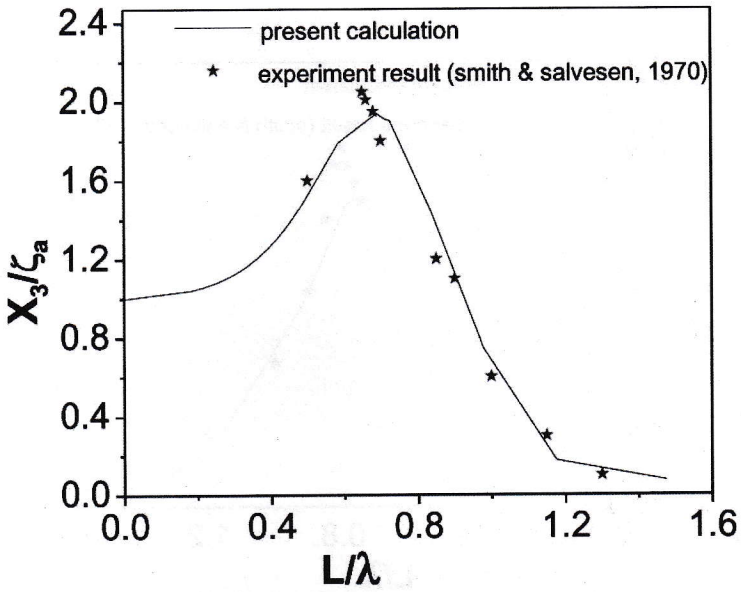

Fig. 15. Heave motion at Fn=0.45 in head sea.

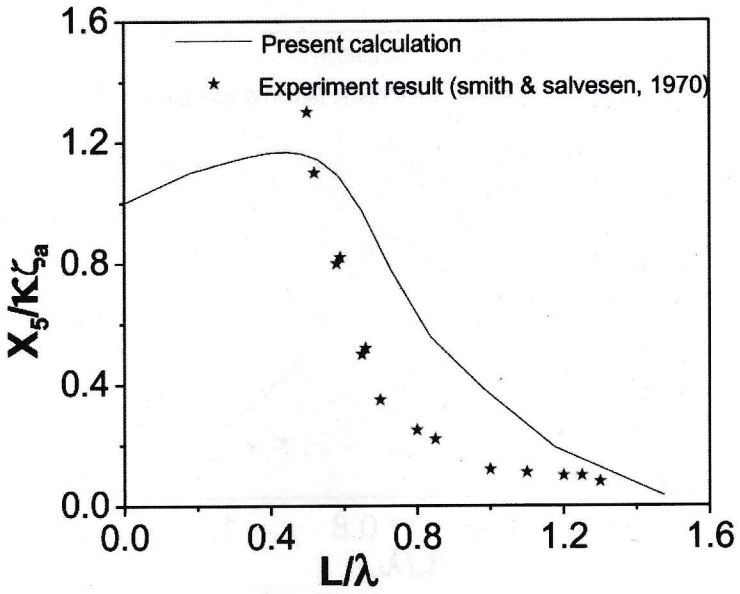

Fig. 16. Heave motion at F_n=0.45 in head sea.

Fig. 16, shows the comparison between the calculated results with experimental results for pitch motion at Fr = 0.45. From this graph it is seen that the non-dimensional pitch motion increases at a certain limit and then decreases gradually with the increase of the value of L/λ and the calculated value is slightly deviates from the experimental value.

4.2. Case study-2: Bulk Carrier

For the validation of numerical results given by developed computer program, a Bulk Carrier of C_B=0.804 has been taken. The principal particulars of the ship are shown in Table 3. Body plan is shown in Fig. 17. Test results have been taken from Salvesen et al. (1970). The NK(3D) and IRS(3D) data have been taken from Zhu et al. (2004).

Table 3. Model Characteristics of bulk carrier.

LWL	4.5m
LBP	4.5m
Beam	0.793m
Draft	0.285m
LCG	0.144m (forward of amidships)
C_B	0.804

shows the comparison between the calculated results with experimental and other numerical results for heave motion at Fr = 0.131 in head sea. From this graph, it is seen that the non-dimensional heave motion increases gradually with the increase of the value of λ/L and the calculated value is close to the experimental value except at higher value of λ/L where the wave length is too high.

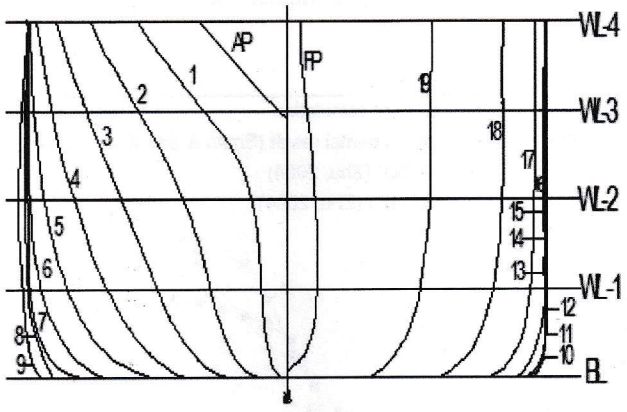

Fig. 17. Body plan of Bulk Carrier.

Fig. 18, shows the comparison between the calculated results with experimental and other numerical results for heave motion at Fr = 0.131 in head sea. From this graph, it is seen that the non-dimensional heave motion increases gradually with the increase of the value of λ/L and the calculated

value is close to the experimental value except at higher value of λ/L where the wave length is too high.

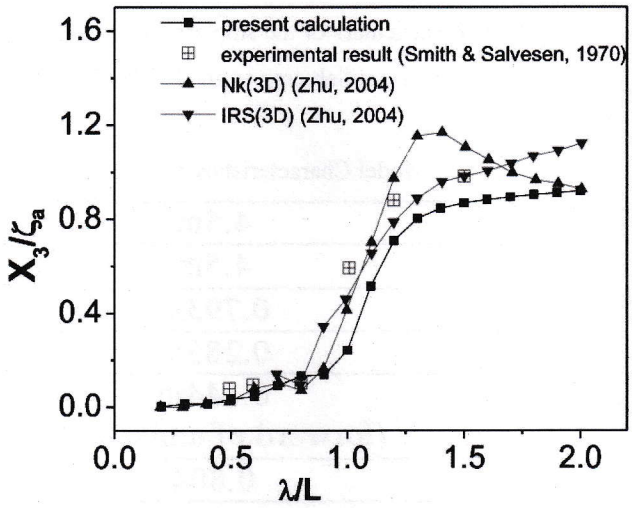

Fig. 18. Heave motion at F_n=0.131 in head sea.

Fig.19, shows the comparison between the calculated results with experimental and numerical results for pitch motion at Fr = 0.131 in head sea. From this graph, it is seen that the non-dimensional pitch motion increases gradually with the increase of the value of λ/L and the calculated value is close to the experimental value except at higher value of λ/L.

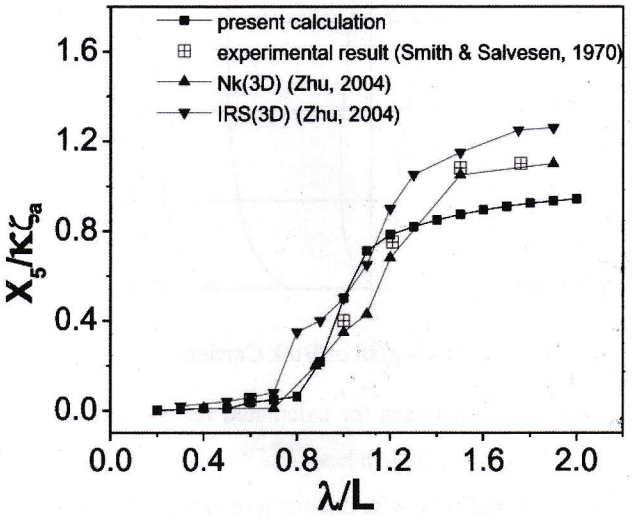

Fig. 19. Peach motion at F_n=0.131 in head sea.

5.0. Conclusion

From the numerical results calculated by the present computer code, the following conclusion may be drawn:

i. The present numerical result slightly deviates from the experimental results, but overall prediction is quite reasonable.

ii. The program gives reasonable results for a wide range hull form ($C_B = 0.50 \sim 0.80$).

iii. As the experimental work is very costly, so this program might be useful for the prediction of ship motion at initial design stage.

References

Al Amin, M.; Masudur, R. (2013). Prediction of Ship Motion in Regular Head Waves, UG thesis, Bangladesh University of Engineering & Technology, Dhaka, Bangladesh.

Crossland, P.; Wilson, P. A.; Bradburn, J.C. (1993) The Free Decay of Coupled Heave and Pitch Motions of Model Frigates, Transactions of the Royal Institution of Naval Architects.

Gerritsma, I.J.; Beukelman, W. (1967) Analysis of the Modified Strip Theory for Calculation of Ship Motions and Wave Bending Moments, Report No. 96S.

Korvin-Kroukovsky, B.V.; Jacobs, W.R. (1957) Pitching and Heaving Motions in Regular Waves, Transactions, Society of Naval Architecture and Marine Engineers.

Liu, Y. L.; Miao, G.P. (1997) An Engineering Prediction Method for Large Amplitude Motions of Ships in Waves, 6th International Offshore and Polar Engineering Conference, vol. 3.

Ogilvie, E.O.; Tuck, T.F. (1969) A Rational Strip Theory of Ship Motions, University of Michigan, Report No. 013.

Salvesen, N.; Tuck, E.O. (1970) Ship Motion and Ship Loads, Transactions, Society of Naval Architecture and Marine Engineers.

Troesch. (1981) Sway, roll and yaw motion coefficients based on a forward-speed slender-body theory-part 1, Journal of Ship Research.

Wang. (1976) Dynamical Theory of Potential Flows with a Free Surface, A Classical Approach to Strip Theory of Ship Motions, Journal of Ship Research.

Zhu, T.; Xu, L.; Singh, SP.; Ha, TB. (2004) A Comparative Study of 3-D Methods with Experimental Results for Seakeeping Analysis, ICHD Conference, Australia.